Pergamon

Available online at www.sciencedirect.com

SCIENCE @ DIRECT®

Cement and Concrete Research 33 (2003) 1825–1830

CEMENT AND CONCRETE RESEARCH

The effects of potassium and rubidium hydroxide on the alkali–silica reaction

K. Shomglin[a,b,*], L. Turanli[b,c], H.-R. Wenk[a], P.J.M. Monteiro[b], G. Sposito[b,d]

[a]*Department of Earth and Planetary Sciences (formerly Geology and Geophysics), University of California, Berkeley, CA 94720, USA*
[b]*Department of Civil and Environmental Engineering, University of California, Berkeley, CA 94720, USA*
[c]*Department of Civil Engineering, Middle East Technical University, Ankara 06531, Turkey*
[d]*Department of Environmental Science, Policy and Management, University of California, Berkeley, CA 94720, USA*

Received 19 March 2002; accepted 9 June 2003

Abstract

Expansion of mortar specimens prepared with an aggregate of mylonite from the Santa Rosa mylonite zone in southern California was studied to investigate the effect of different alkali ions on the alkali–silica reaction in concrete. The expansion tests indicate that mortar has a greater expansion when subjected to a sodium hydroxide bath than in a sodium–potassium–rubidium hydroxide bath. Electron probe microanalysis (EPMA) of mortar bars at early ages show that rubidium ions, used as tracer, were present throughout the sample by the third day of exposure. The analysis also shows a high concentration of rubidium in silica gel from mortar bars exposed to bath solutions containing rubidium. The results suggest that expansion of mortar bars using ASTM C 1260 does not depend on the diffusion of alkali ions. The results indicate that the expansion of alkali–silica gel depends on the type of alkali ions present. Alkali–silica gel containing rubidium shows a lower concentration of calcium, suggesting competition for the same sites.

Keywords: Alkali–aggregate reaction; Aggregate; KOH; Microstructure; SEM

1. Introduction

Surface and colloid science has been recognized by some researchers as being important in understanding some of the phenomena that occur in concrete [1–5]. Surface characteristics of materials tend to be different than bulk properties because of the unsatisfied surface charges. If these surfaces come into contact with other surfaces (such as other solids or liquids), the surface charges change the properties of these phases [2].

Surface charge can affect the thickness of adsorbed layers of water and ions [3]. As the thickness of these layers changes, so does the volume of the particle, creating swelling and compressive behavior. Because the expansive alkali–silica reaction product is believed to be a colloidal system, it could be possible to use double-layer theories to explain its behavior [4].

One method to test for alkali–silica reactivity is the ASTM C 1260, where mortar bars are immersed into a hydroxide bath at an elevated temperature. However, this test only uses sodium as alkali ion. To verify the predictions of the double-layer theory about the ion effect on changes in volume, the results of the ASTM C 1260 test were compared to a test that included a mixture of sodium and potassium ions. Rubidium ions were also added as a marker because sodium and potassium are present both in the aggregate and cement paste, and are therefore difficult to track. Electron probe microanalysis (EPMA) was used to investigate whether the alkali–silica gel preferentially adsorbs certain ions over others.

2. Materials and experimental methods

The rock used for testing was a mylonite collected from the upper Palm Canyon area of the Santa Rosa mylonite zone. This metamorphic rock is composed of gray and white bands, which represent compositional layering formed through the reduction of grain size and recrystallization due to ductile deformation. Feldspar augen are common in the matrix of fine-grained quartz and biotite. Quartz grains have a grain size ranging from a few micrometers to 50 μm, biotite from a few micrometers to 10 μm, and plagioclase from 0.5 to 1 mm.

---

* Corresponding author. Department of Earth and Planetary Sciences, University of California, Berkeley, CA 94720, USA.

E-mail address: roketman@uclink4.berkeley.edu (K. Shomglin).

0008-8846/$ – see front matter © 2003 Elsevier Ltd. All rights reserved.
doi:10.1016/S0008-8846(03)00204-7

A petrographic thin section is shown in Fig. 1. Biotite and quartz exhibit strong preferred orientation. Foliation and lineation can be observed in hand samples.

Type I/II Portland cement was used. The oxide percent composition is: CaO, 64.72; SiO_2, 21.24; Fe_2O_3, 3.82; Al_2O_3, 3.57; MgO, 1.69; P_2O_5, 0.32; TiO_2, 0.31; Na_2O, 0.18; K_2O, 0.10; Cr_2O_3, 0.04; Mn_2O_3, 0.04; SO_3, 2.27.

Two different tests were used on the same rock and cement combinations: a traditional test [6] and a modified ASTM C 1260 test. The only difference between these two tests is in the bath solution composition. Whereas the traditional ASTM C 1260 test requires a bath solution containing 1 M sodium hydroxide, the modified test bath solution contained sodium hydroxide, potassium hydroxide, and rubidium hydroxide. A ratio of 3:1 potassium hydroxide to sodium hydroxide was used to find out the effects of high potassium concentration on the expansion. The combined concentration of potassium hydroxide and sodium hydroxide totaled 0.7 M. Rubidium hydroxide was also added to the modified test at a concentration of 0.3 M to bring the total concentration of hydroxide to 1 M. Rubidium was chosen because it does not exist in cement or aggregates and is therefore relatively easy to detect. Rubidium ions can then be used to track alkali distribution in the specimen throughout the duration of the test.

The rock to be used as aggregate was crushed and graded according to ASTM C 1260. Nine mortar bars were made for each test, with four out of the nine bars designated as the control group. The mortar bars were cured for 24 h in a fog room at 21 ± 2 °C, demolded, and immersed in water and heated to 80 °C. After 24 h, the length of the control specimens was measured. All mortar bars except one were then immersed in a closed container of 1 M sodium hydroxide solution maintained at 80 °C. The excluded mortar bar was designated as “zero day” specimen. On the 10th, 20th, and 30th days, a mortar bar was removed and excluded from the chemical bath.

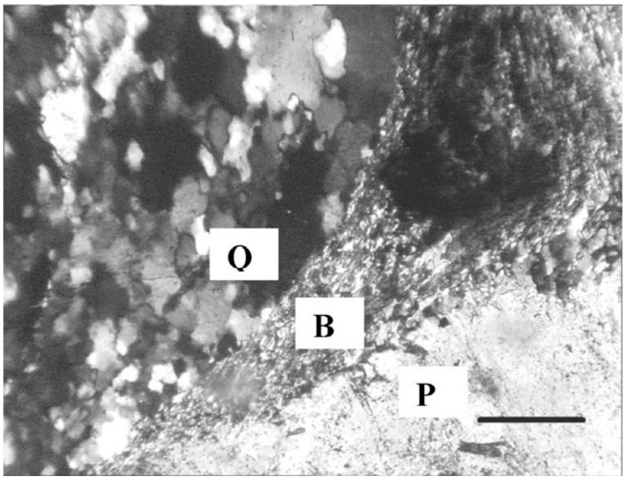

Fig. 1. Petrographic thin section showing the three major minerals that are found in Santa Rosa mylonite: P, plagioclase; B, biotite; and Q, quartz. Scale bar = 50 μm.

From these excluded bars, a cross section with a thickness of 12.7 mm along the length of the bar was removed using a rock saw. These sections were left in a vacuum for a week before being impregnated with Epotek epoxy under vacuum. The molds that held the specimen and the epoxy were circular (25.4 mm in diameter) and designed to fit the sample holder for EPMA. After the epoxy cured, the sample was polished with a final grit of 1/4-μm diamond polishing compound. Because the reaction product is water sensitive, kerosene-based polishing compounds were used during polishing.

Chemical analysis and images of the specimens were taken using a Cameca SX-51 microprobe instrument running at 15 kV with a beam current of 20 nA. For all samples, the beam size was 5 ìm, and for analyses, the time exposed to the beam was 100 s. Using a set of external standards, the wavelength dispersive X-ray spectrometers were set up to analyze simultaneously for 10 elements: Al, Ca, Fe, K, Mg, Na, O, Rb, S, and Si. The oxygen is then combined with the other elements and the oxide compositions are calculated. The excess oxygen can be used to estimate the amount of water present in the sample. This is only an approximation because it assumes that no water was lost during epoxy impregnation under vacuum, no water was introduced or lost during polishing, no water was lost through heating when applying a carbon coating to the sample prior to analysis, no carbonation occurred, and no water was lost during the analysis as the electron beam heats up the sample.

Backscattered electron (BSE) images were taken of the samples using EPMA. In addition to providing an image of the sample, BSE images may also provide insight into the chemical composition through the observed contrast. An area of dark image indicates that few electrons were backscattered, and therefore has low electron density and is composed of low atomic number elements. As the electron density of an area of the sample increases (heavier elements), a greater number of electrons are backscattered and produce the bright areas of the image.

3. Results and discussion

Fig. 2 shows the results of both the ASTM C 1260 and the modified test that includes a mixture of sodium, potassium, and rubidium ions in the bath solution. It was found that mortar bars exposed to a bath solution containing only sodium hydroxide had a greater expansion than mortar bars exposed to a sodium–potassium–rubidium hydroxide bath.

Mortar bars were sectioned before immersion into the hydroxide bath and at 10, 20, and 30 days after immersion. These are shown in Fig. 3A–D, respectively.

The image of a section before being immersed in a hydroxide bath (Fig. 3A) shows a polycrystalline aggregate of quartz in the center. The condition of this quartz cluster is

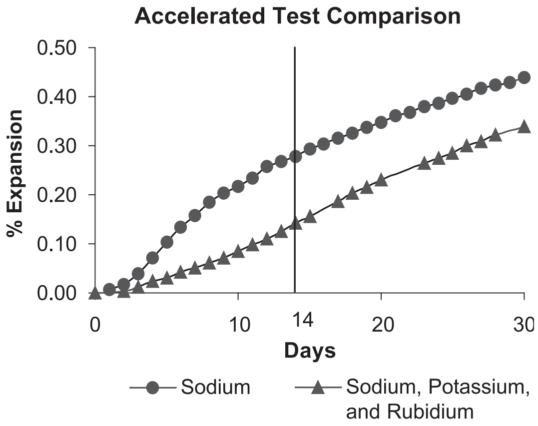

Fig. 2. Expansion of mortar bars immersed in 1 M NaOH (ASTM C 1260) and 0.525 M KOH + 0.175 M NaOH + 0.3 M RbOH (modified).

representative of the condition of other quartz clusters seen in the mortar bar, showing no cracks or fissures, and having rough edges that are caused by the aggregate-preparation process (crushing). The image of a section after 10 days of immersion in a hydroxide bath (Fig. 3B) shows that cracks have begun to propagate, signalling that a reaction is occurring. This reaction is observed as an expansion of the mortar bar (Fig. 2). By the 20th day (Fig. 3C), the quartz regions have become extensively deteriorated, with cracks and pits joining to form large fissures while other mineral constituents of the aggregate such as feldspar and biotite remain unchanged. This condition is even more evident after 30 days (Fig. 3D). Alkali–silica gel could be found within these cracks, as well as in air voids within the mortar by the 30th day (Fig. 4).

The migration of the rubidium, potassium, and sodium ions from the bath solution into the mortar bar was tracked by using EPMA to perform chemical analysis on samples of different ages, traversing from the center of the sample towards the outside edge (Fig. 5).

The clearest indication that alkali ions are able to migrate to the center of the sample can be seen in the rubidium profile. Because rubidium is not present in any phase of the samples, its presence at 3 days is solely due to the diffusion of rubidium from the chemical bath into the sample. It was also found that the concentration of potassium and sodium had also increased. This indicates that the migration of alkali

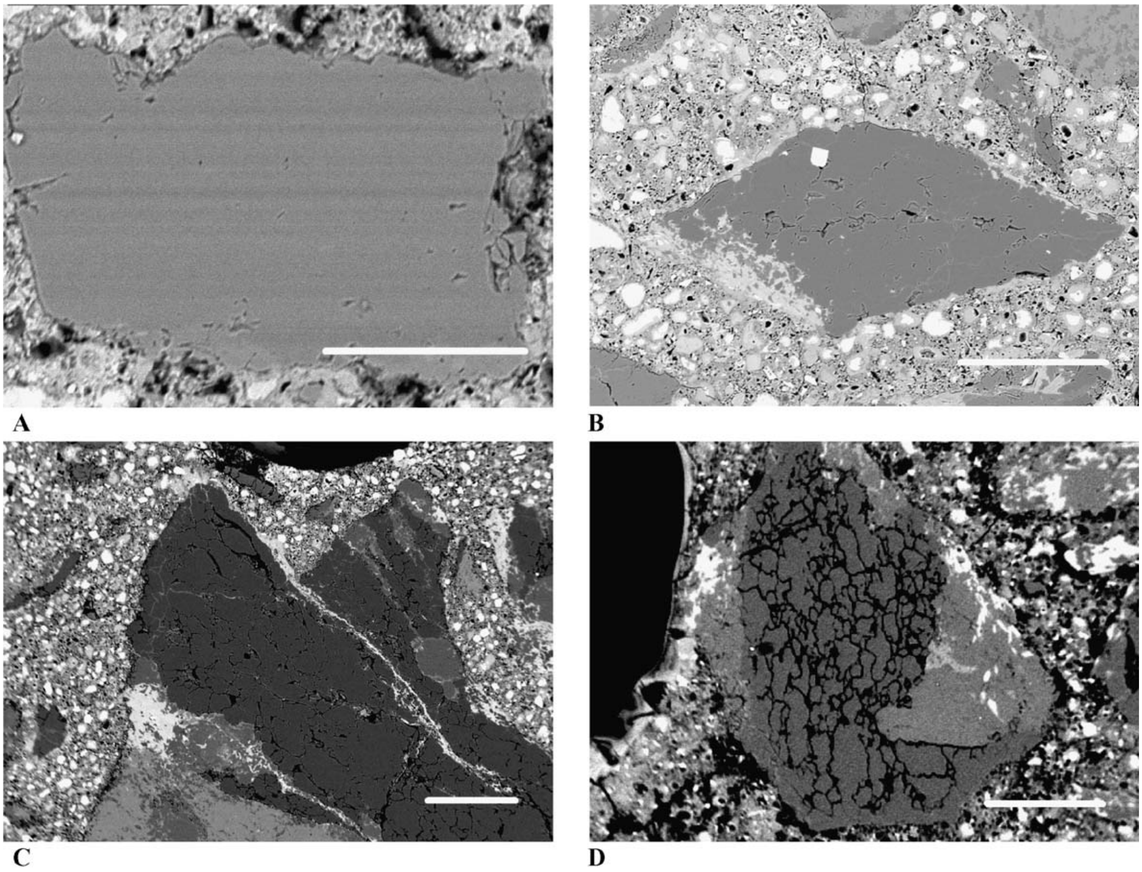

Fig. 3. BSE images of sections taken from mortar bars showing the evolution of polycrystalline quartz clusters. (A) Before immersion into a hydroxide bath: a cluster of quartz surrounded by hydrated cement paste. Damage of the quartz aggregate is confined to the outer edges as a result of the aggregate-preparation process. The condition is representative of the other quartz clusters found in the mortar bar at this age. Scale bar = 100 μm. (B) 10 days: a quartz cluster that has begun to deteriorate, exhibiting cracking. Scale bar = 100 μm. (C) 20 days: extensive deterioration of quartz regions. Scale bar = 250 μm. (D) 30 days: a highly deteriorated quartz cluster. Scale bar = 250 μm.

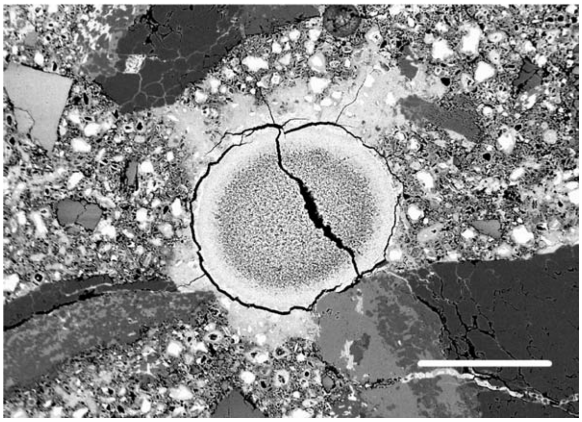

Fig. 4. BSE image of a section taken from a mortar bar 30 days after immersion in a hydroxide bath showing an air void filled with alkali–silica gel. Scale bar = 250 μm.

ions through the mortar is fast. The mortar does not act as a barrier that effectively prevents appreciable diffusion of alkali ions. This verifies that for the ASTM C 1260 test, the expansion of the mortar bars is not dependent on the diffusion of the alkali ions through the mortar bar, but rather, expansion depends on other parameters such as the degree of reactivity of the aggregate.

By the 10th day, the cement matrix was developed sufficiently for different distinct phases (i.e., CSH, ASR gel, and a few partially hydrated cement particles) to be large enough for analysis. These areas, as well as the transition zone between the aggregate and the cement paste, were also analyzed. It was found that rubidium was no longer present in the cement paste, but was to be found along the interfacial zone between the aggregate and cement matrix. This confirms that the quartz could act as a sink for rubidium and other alkali ions.

The difference in the degree of expansion depending on which alkali ions are present can be explained by using double-layer theories, which some researchers have used to predict and explain the behavior of alkali–silica gel [7–10]. The dependence of expansion on different alkali ions can be explained by the larger hydrated radius of Na^+ compared to K^+ and Rb^+ ions (Table 1). Because sodium ions have a larger hydrated radius than potassium and rubidium ions, it is expected that sodium-rich alkali–silica gels would have a greater expansion than those low in sodium (rich in potassium and/or rubidium). Other researchers have found that sodium showed a higher efficiency than potassium in causing expansion when the aggregate is reactive [11,12].

To verify that the alkali–silica gels from the two different experiments had different compositions, quantitative chemical analysis was performed using EPMA, and the results are listed in Table 2. These show that the alkali–silica gel produced from the two different chemical baths have different chemical compositions, one rich in sodium and the other rich in rubidium and potassium. From the results listed in Table 2, the sodium-rich gel had a greater expansion than the potassium- and rubidium-rich gel, verifying the double-layer theories prediction.

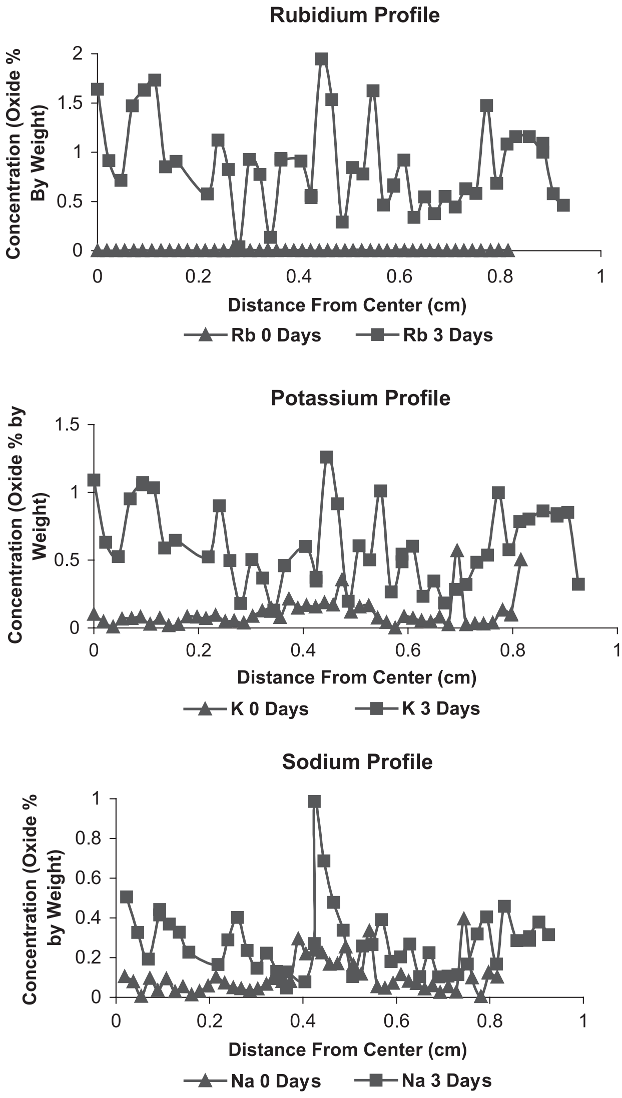

Fig. 5. EMPA for Rb, K, and Na across a section of a mortar bar before immersion (0 days) and after immersion for 3 days in a chemical bath containing 0.525 M KOH + 0.175 M NaOH + 0.3 M RbOH.

The chemical analysis also suggests that when rubidium is present, the reaction product incorporates appreciable quantities of rubidium into it. It is possible that the rubidium ion can most easily bind to the silica sites because it has the most diffuse charge on its surface. This allows for rubidium

Table 1
Ionic and hydrated radii of ions in water [5,13,14]

Ion	Ionic radius (nm)	Hydrated radius (nm)
Na^+	0.095	0.36
K^+	0.133	0.33
Rb^+	0.152	0.29
Ca^{+2}	0.099	0.41

Table 2
Average chemical composition of alkali–silica gel formed in samples prepared with different alkali hydroxides at an initial molar concentration equal to 1

Samples	1 M NaOH at 30 days	0.525 M KOH + 0.175 M NaOH + 0.3 M RbOH at 30 days
Expansion % at 30 days	0.44	0.33
Chemical composition of gels obtained by electron probe microanalysis (%wt. oxide)		
SiO_2	64.4 ± 2.7	62.1 ± 1.8
CaO	16.8 ± 1.8	9.9 ± 2.3
Na_2O	4.0 ± 1.0	2.8 ± 1.2
K_2O	1.8 ± 0.72	5.5 ± 0.82
Rb_2O	–	12.0 ± 0.65

ions to be the least hydrated so that it has a smaller hydrated sphere than other ions to be removed before interacting with the silica sites.

It is also shown that there is a reduction in the calcium concentration of the alkali–silica gel when potassium and rubidium ions are added to the chemical bath. This suggests that it is more difficult for calcium ions to replace the more tightly bound rubidium and potassium ions than for calcium ions to replace the more loosely held sodium ions in the alkali–silica-gel structure. Although calcium ions carry a charge of +2 and are therefore more attracted to the negative silica sites, the small size and the high charge of calcium combine to give it a large hydrated sphere of water that have to be overcome before binding occurs to the silica. It is possible that potassium or rubidium ions have a small-enough hydrated sphere that they decrease the amount of calcium exchange.

The possibility that the expansion of silica gel can vary with the addition of different compounds has been the subject of many studies since the discovery of ASR in the 1940s, the first of which dates back more than 50 years [15]. It was not until the 1980s and 1990s that commercial use of lithium compounds were explored and developed [16]. It was found that high doses of these compounds are required to be effective because as much as half of the lithium ions are adsorbed by the formation of cement hydration products [17]. The mechanism by which these compounds suppress ASR is not clearly known. It has been suggested that lithium silicates could be more stable and less expansive than sodium or potassium silica gels [16,18]. It is also possible that the presence of lithium decreases the rate of silica dissolution [19].

A potential problem that can result from adding insufficient amounts of some lithium compounds includes an increase in expansion as compared to when none is added. However, some lithium compounds such as $LiNO_3$ do not have such consequences and are being studied [20]. Overall, it is still not known what the long-term effects of using lithium compounds will be on the environment and on concrete.

4. Conclusion

Results of a test slightly modifying ASTM C 1260 to replace the 1 M sodium hydroxide storage solution with a solution containing sodium, potassium, and rubidium hydroxide showed that within the same time periods, gels containing a mixture of sodium, potassium, and rubidium expanded less than gels containing only sodium.

BSE images reveal the progression of the deterioration of quartz due to the alkali–silica reaction. However, it is unclear whether there is any preference as to where on the grain the reaction develops and proceeds. It is possible that the reaction follows along areas of high energy, such as grain boundaries and areas of high dislocation densities.

Quantitative chemical analysis using EPMA showed that already at early ages, rubidium ions were present throughout the whole sample. This indicates that the migration of rubidium ions and other alkali ions through the mortar bar is fast. The mortar does not act as a significant barrier on the diffusion of alkali ions. Therefore, the alkali–silica reaction that occurs in these mortar bars is not dependent on the diffusion of alkali ions from outside of the bar. Because this occurs at a fast rate, the rate of reaction of alkali and unstable silica determines the rate of expansion. It was shown that at later stages, rubidium could only be found along the aggregate boundaries. This confirms that quartz acts as a sink for rubidium and other alkali ions.

Chemical analysis also indicates that alkali–silica gels containing potassium and rubidium have a low calcium content. The hydrated size of potassium and rubidium ions could be small enough for them to be tightly held to the gel and not be easily replaced by calcium, whereas sodium ions could more easily be replaced by calcium because their hydrated size is too large.

Further study of rubidium compounds may show ASR suppression. Although they may not be as effective as lithium compounds, it would still be interesting to see what effect these compounds have on the silica gel.

Acknowledgements

Paulo Monteiro wishes to acknowledge the financial support given by NSF and the Federal Highway Administration (Award CMS-9812757). The helpful discussions with Dr. Richard Livingston are appreciated.

We also acknowledge the assistance of John Donovan with microprobe analysis.

References

[1] R.J. Hunter, Foundations of Colloid Science, Oxford Univ. Press, New York, 2001.

[2] J.O'M. Bockris, A.K.N. Reddy, Modern Electrochemistry, Plenum, New York, 1970.

[3] G. Sposito, The Surface Chemistry of Soils, Oxford Univ. Press, New York, 1984.

[4] K.H. Tan, Principles of Soil Chemistry, Marcel Dekker, New York, 1982.

[5] J. Israelachvili, Intermolecular and Surface Forces, Academic Press, New York, 1992.

[6] American Society for Testing and Materials (ASTM), Standard test method for potential alkali reactivity of aggregates (Mortar-Bar Method), ASTM C 1260-94, Annual Book of ASTM Standards, vol. 04.02, 1994, Philadelphia.

[7] F.A. Rodrigues, P.J.M. Monteiro, G. Sposito, The alkali–silica reaction—the effect of monovalent and bivalent cations on the surface charge of opal, Cem. Concr. Res. 31 (11) (2001) 1549–1552.

[8] F.A. Rodrigues, P.J.M. Monteiro, G. Sposito, Surface charge density of silica suspended in water–acetone mixtures, J. Colloid Interface Sci. 211 (2) (1999) 408–409.

[9] M. Prezzi, P.J.M. Monteiro, G. Sposito, Alkali–silica reaction: Part 1. Use of the double-layer theory to explain the behavior of the reaction product gels, ACI Mater. J. 94 (1) (1997) 10–17.

[10] M. Prezzi, P.J.M. Monteiro, G. Sposito, Alkali–silica reaction: Part 2. The effect of chemical additives, ACI Mater. J. 95 (1) (1998) 3–10.

[11] J.H.P. van Aardt, S. Visser, Progress report: Part 2. CSIR Research Report BBR 577 Petroria (1982) 1–5.

[12] R.E. Oberholster, G. Davies, An accelerated method for testing the potential alkali reactivity of siliceous aggregates, Cem. Concr. Res. 16 (2) (1986) 181–189.

[13] J.L. Fulton, D.M. Pfund, S.L. Wallen, M. Newville, E.A. Stern, Y. Ma, Rubidium ion hydration in ambient and supercritical water, J. Chem. Phys. 105 (6) (1996) 2161–2166.

[14] D.R. Lide, The Chemical Rubber Company Handbook of Chemistry and Physics, The Chemical Rubber Publishing, Boca Raton, FL, 2000.

[15] W.J. McCoy, A.G. Caldwell, A new approach to inhibiting alkali–aggregate expansion, J. Am. Concr. Inst. 22 (9) (1951) 693–706.

[16] D.C. Stark, Lithium salt admixtures—an alternative method to prevent expansive alkali–silica reactivity, Proceedings of the 9th International Conference on Alkali–Aggregate Reaction, London, 1992, pp. 1017–1025.

[17] S. Ong, Study of LiOH, NaOH, and KOH on alkali–silica reaction, MSCE thesis, School of Civil Engineering, Purdue University, 1990.

[18] M. Lawrence, H.F. Vivian, The reactions of various alkalis with silica, Aust. J. Appl. Sci. 12 (1) (1961) 96–103.

[19] P.W.J.G. Wijnen, T.P.M. Beelen, J.W. de Haan, C.P.J. Rummens, L.J.M. van de Ven, R.A. van Saten, Silica gel dissolution in aqueous alkali metal hydroxides studied by 29Si-NMR, J. Non-Cryst. Solids 109 (1989) 85–94.

[20] S. Diamond, Unique response of $LiNO_3$ as an alkali–silica reaction—preventive admixture, Cem. Concr. Res. 29 (1999) 1271–1275.